

# DYNAMIC DEPOLARIZATION OF INTERACTING FLUOROPHORES

## Effect of Internal Rotation and Energy Transfer

FUMIO TANAKA

*Mie Nursing College, Torii-cho 100, Tsu, Mie, Japan 514*

NOBORU MATAGA

*Department of Chemistry, Faculty of Engineering Science, Osaka University, Toyonaka, Osaka, Japan 560*

**ABSTRACT** Effects of internal rotation on the fluorescence decay functions and time-dependent anisotropies of fluorophores bound to a spherical macromolecule are theoretically investigated in the presence of the intramolecular energy transfer interaction by solving relevant rotational diffusion equations. The model system examined is one in which the energy donor is internally rotating around an axis fixed at the macromolecule and the acceptor is fixed at a definite position in the macromolecule. The effect of internal rotation in the system is described by Hill's functions with two cosine terms. The fluorescence decay function and anisotropy decay are functions of the ratio of energy-transfer probability averaged over the internal rotation angle to the rotary diffusion co-efficient. When the internal rotation is much faster than energy transfer, the decay function of the donor is predicted to be a single exponential, and the anisotropy decay is essentially described by the expression derived by Gotlieb and Wahl (1963. *J. Chim. Phys.* 60:849–856). However, deviation from it becomes pronounced as the rotation becomes slower. Methods of numerical analysis are presented for decay function and anisotropy decay, as well as relative quantum yield and polarization anisotropy under steady-state excitation, and examined for a simplified system under the variation of the diffusion coefficient.

### INTRODUCTION

Since Perrin's classic work (1936), rotational movement of an isolated fluorophore has been investigated by the depolarization method. The method had been developed in the field of biochemistry (Weber, 1952). Theoretical studies on the time-dependent depolarization due to rotational Brownian motion have been made for spherical molecules (Jabłoński, 1961), rotational ellipsoids (Lombardi and Dafforn, 1966) and for a completely asymmetric rotor (Tao, 1969; Weber, 1971; Belford et al., 1972; Ehrenberg and Rigler, 1972; Chuang and Eisenthal, 1972). The anisotropy of a small fluorophore covalently bound to a spherical macromolecule was also worked out by Gotlieb and Wahl (1963), and applied to obtain the rotational diffusion coefficient of proteins (Wahl and Weber, 1967; Knopp and Weber, 1969; Brochon and Wahl, 1972; Wahl, 1975b). In particular, measurements of the anisotropy decay (Munro et al., 1979) or lifetime-resolved fluorescence anisotropy (Lakowicz and Cherek, 1980; Lakowicz and Weber, 1980) have revealed structural mobility in proteins in the nanosecond time scale.

On the other hand, excitation energy transfer also brings about the depolarization even if the fluorescent molecules

are fixed in rigid solution (Tanaka and Mataga, 1979). The mechanism of energy transfer due to dipole-dipole interaction has been established by Förster (1948) and subsequent workers (Latt et al., 1965; Mataga et al., 1967, 1969; Stryer and Haugland, 1967; Haugland et al., 1969). The rate of the energy transfer following Förster's mechanism depends on the intermolecular distance between the donor and acceptor and on the mutual orientation between their transition dipole moments (Förster, 1951). Analysis of the energy-transfer interaction has been used to evaluate intermolecular distance in proteins (Stryer, 1978). However, because of the dependence of critical transfer distance on the orientation factor, certain arbitrariness for the obtained intermolecular distance cannot be avoided. Dale and Eisinger (1975) attempted to establish a method for evaluating the intermolecular distance from the energy-transfer rate and the fluorescence depolarization factor.

Despite its importance, however, a quantitative treatment for the fluorescence decay function as well as anisotropy decay of the fluorophores internally rotating around a fixed axis has never been worked out during the energy-transfer interaction. In this work, we formulate the expressions for the fluorescence decay curve and anisotropy

decay in a model system, where the energy donor rotates around a fixed axis and the acceptor is fixed in a definite direction relative to the rotating axis of the donor within a spherical molecule.

### ROTATIONAL DIFFUSION EQUATIONS WITH ENERGY TRANSFER INTERACTION

The geometrical arrangement of the molecular system and experimental laboratory system is illustrated in Fig. 1. A spherical molecule possesses a microscopic molecular system ( $x y z$ ) and macroscopic laboratory system ( $X Y Z$ ). Both coordinate systems are connected by Euler angles ( $\psi \theta \gamma$ ). Transition dipole moments of absorption and emission of the energy donor are denoted by  $\mathbf{m}_{1a}$  and  $\mathbf{m}_{1e}$ , respectively, and those of the acceptor,  $\mathbf{m}_{2a}$  and  $\mathbf{m}_{2e}$ .  $\mathbf{m}_{1a}$  and  $\mathbf{m}_{1e}$  rotate with a rotational diffusion coefficient of  $D_R$  around the  $z$ -axis with latitudinal angles of  $\delta_a$  and  $\delta_e$ , respectively. The rotation variable of  $\mathbf{m}_{1e}$  in the  $xy$ -plane is represented by  $\phi$ . The angle between the projections of  $\mathbf{m}_{1a}$  and  $\mathbf{m}_{1e}$  onto  $xy$ -plane is  $\epsilon$ . The distance vector between the centers of the donor and the acceptor is given by  $\mathbf{R}$ , which

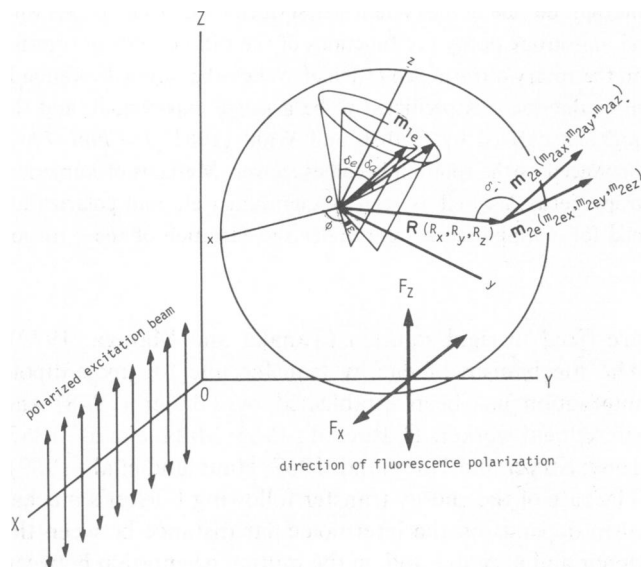


FIGURE 1 Geometric arrangement of experimental and molecular systems. The laboratory and molecular systems are represented by coordinate systems ( $X Y Z$ ) and ( $x y z$ ), respectively. The two systems are related to each other through a rotation matrix with Eulerian angles ( $\theta \psi \gamma$ ). An incident beam polarized from the direction of the  $X$ -axis in the  $Z$ -direction excites a sample at 0. Fluorescence from the sample is observed in the  $Y$ -direction through filters polarized along the  $Z$  ( $F_Z$ ) and the  $X$ -axes ( $F_X$ ). Spherical macromolecules processing both an energy donor and an acceptor are being considered. Transition dipole moments of absorption and emission of the donor are  $\mathbf{m}_{1a}$  and  $\mathbf{m}_{1e}$ , respectively. The angle between the projection of these vectors on the  $XY$  plane and the  $X$ -axis is denoted by  $\phi$ . Co-latitude angles of  $\mathbf{m}_{1a}$  and  $\mathbf{m}_{1e}$  are  $\delta_a$  and  $\delta_e$ , respectively, and differences between their  $\phi$  values is  $\epsilon$ . The distance between the energy acceptor and donor is  $\mathbf{R}(R_x, R_y, R_z)$ , where  $R_x, R_y$ , and  $R_z$  are the direction cosines of  $\mathbf{R}$ . Transition dipole moments of the acceptor absorption and emission are  $\mathbf{m}_{2a}$  ( $m_{2ax}, m_{2ay}, m_{2az}$ ). An angle between  $\mathbf{R}(R_x, R_y, R_z)$  and  $\mathbf{m}_{2a}$  ( $m_{2ax}, m_{2ay}, m_{2az}$ ) is  $\delta$ . The polarized light excites only the donor chromophore.

may be defined with directional cosines,  $\mathbf{R}/R = (R_x, R_y, R_z)$ . The vectors of transition dipole of acceptor are fixed at certain directions,  $\mathbf{m}_{2a} = (m_{2ax}, m_{2ay}, m_{2az})$  for the absorption and  $\mathbf{m}_{2e} = (m_{2ex}, m_{2ey}, m_{2ez})$  for the emission. The donor molecule is excited with a polarized beam along the  $Z$ -axis in the direction of the  $X$ -axis. Emission from the donor or acceptor is observed in the direction of the  $Y$ -axis through a polarization filter along  $Z$ -axis or  $X$ -axis.

The diffusion equations for the donor and the acceptor that are interacting with each other are given by Eqs. 1 and 2,

$$\frac{\partial \rho_1(\psi \theta \phi t)}{\partial t} = -\{k_1 + k_t(\phi)\}\rho_1(\psi \theta \phi t) + DL\rho_1(\psi \theta \phi t) + D_R \frac{\partial^2 \rho_1(\psi \theta \phi t)}{\partial \phi^2} \quad (1)$$

$$\frac{\partial \rho_2(\psi \theta \phi t)}{\partial t} = -k_2\rho_2(\psi \theta \phi t) + DL\rho_2(\psi \theta \phi t) + k_t(\phi)\rho_1(\psi \theta \phi t), \quad (2)$$

where  $\rho_1(\psi \theta \phi t)$  and  $\rho_2(\psi \theta \phi t)$  denote probabilities of the excitation of donor and acceptor;  $k_1, k_2$ , and  $k_t(\phi)$  are rate constants of the excited state decay of donor ( $k_1$ ) and acceptor ( $k_2$ ) in the absence of the interaction, and of energy transfer from the donor to the acceptor [ $k_t(\phi)$ ], which is dependent on  $\phi$ , respectively. Diffusion coefficients of the rotational motion of the entire molecule and internal motion are respectively designated by  $D$  and  $D_R$ . Differential operator  $L$  is the angular part of Laplacian,

$$L \equiv \frac{\partial^2}{\partial \theta^2} + \cot \theta \frac{\partial}{\partial \theta} + \frac{1}{\sin^2 \theta} \cdot \frac{\partial^2}{\partial \psi^2}. \quad (3)$$

$k_t(\phi)$  may be expressed by Eq. 4 according to Förster (1951),

$$k_t(\phi) = k_a + k_b \cos(\phi - \alpha) + k_c \cos 2(\phi - \alpha), \quad (4)$$

where

$$k_a = k_1(R_0/R)^6 (1/2) \{\sin^2 \delta_e (1 + 3 \cos^2 \delta - C^2) + \cos^2 \delta_e C^2\} \quad (5)$$

$$k_b = k_1(R_0/R)^6 \sin 2\delta_e C \sqrt{1 + 3 \cos^2 \delta - C^2} \quad (6)$$

$$k_c = (k_1/2)(R_0/R)^6 \sin^2 \delta_e (1 + 3 \cos^2 \delta - C^2) \quad (7)$$

and

$$C = m_{2az} + 3 \cos \delta \cdot R_z. \quad (8)$$

$\delta$  is an angle between the vectors of  $\mathbf{R}$  and  $\mathbf{m}_{2a}$  (see Fig. 1), and  $R_0$  represents the critical transfer distance with an orientation factor equal to one.  $\alpha$  is a phase angle expressed by Eq. 9,

$$\cos \alpha = \frac{m_{2ax} + 3 \cos \delta R_x}{\sqrt{1 + 3 \cos^2 \delta - C^2}}. \quad (9)$$

$\rho_1(\psi \theta \phi t)$  may be solved by using Green's function (Chuang and Eisenthal, 1972),  $G_1(\psi_0 \theta_0 \phi_0 | \psi \theta \phi, t)$  as follows:

$$\rho_1(\psi \theta \phi, t) = \int_0^{2\pi} d\phi_0 \int_0^{2\pi} d\psi_0 \sin \theta_0 d\theta_0 M_{1az}^2(\psi_0 \theta_0 \phi_0) G_1(\psi_0 \theta_0 \phi_0 | \psi \theta \phi, t) \quad (10)$$

where  $M_{1az}(\psi_0 \theta_0 \phi_0)$  represents transition moment of donor absorption excited at  $t = 0$  with polarized beam along Z-axis.  $G_1(\psi_0 \theta_0 \phi_0 | \psi \theta \phi, t)$  describes the rotation of the dipole vector of the donor from  $(\psi_0 \theta_0 \phi_0)$  at  $t = 0$  into  $(\psi \theta \phi)$  at  $t = t$ , and may be expanded in terms of spherical harmonics  $Y_n^m(\theta \psi)$  and an orthonormal function of  $\phi$ ,  $g_s(\phi)$ ,

$$G_1(\psi_0 \theta_0 \phi_0 | \psi \theta \phi, t) = \sum_n \sum_m \sum_s c_{ns}(t) Y_n^{m*}(\theta_0 \psi_0) Y_n^m(\theta \psi) g_s^*(\phi_0) g_s(\phi) \quad (11)$$

with the initial condition

$$\begin{aligned} G_1(\psi_0 \theta_0 \phi_0 | \psi \theta \phi, 0) \\ = \sum_n \sum_m \sum_s Y_n^{m*}(\theta_0 \psi_0) Y_n^m(\theta \psi) g_s^*(\phi_0) g_s(\phi) \\ = \delta(\cos \theta_0 - \cos \theta) \delta(\psi_0 - \psi) \delta(\theta_0 - \phi). \end{aligned} \quad (12)$$

In a similar way,  $\rho_2(\psi \theta \phi t)$  can be expressed also by a Green function,  $G_2(\psi_0 \theta_0 | \psi \theta, t - \tau)$ , and  $\rho_1(\psi \theta \phi t)$ .

$$\rho_2(\psi \theta \phi t) = \int_0^{2\pi} d\psi_0 \int_0^\pi \sin \theta d\theta_0 \int_0^t d\tau k_t(\phi) \rho_1(\psi_0 \theta_0 \phi_0 \tau) G_2(\psi_0 \theta_0 | \psi \theta, t - \tau). \quad (13)$$

$G_2(\psi_0 \theta_0 | \psi \theta, t - \tau)$  can be expressed in terms of spherical harmonics,

$$G_2(\psi_0 \theta_0 | \psi \theta, t - \tau) = \sum_n \sum_m d_n(t - \tau) Y_n^{m*}(\theta_0 \psi_0) Y_n^m(\theta \psi). \quad (14)$$

#### INTERNAL ROTATION DESCRIBED BY HILL'S FUNCTION

The explicit form of the orthonormal function  $g_s(\phi)$  is dependent on  $k_t(\phi)$  in Eq. 4. The general equation for  $g_s(\theta)$  may be described by a kind of Hill's equation as follows (Magnus and Winkler, 1979),

$$\frac{d^2 g_s}{d\chi^2} + \left\{ a_s - 2Q_1 \cos 2\left(\chi - \frac{\alpha}{2}\right) - 2Q_2 \cos 4\left(\chi - \frac{\alpha}{2}\right) \right\} g_s = 0, \quad (15)$$

where  $\chi = \phi/2$  and

$$Q_1 = \frac{2k_b}{D_q} \quad (16)$$

$$Q_2 = \frac{2k_c}{D_q}. \quad (17)$$

$g_s$  is a Hill function with two cosine terms and is represented as an infinite series of cosine function or sine function of  $(\chi - \alpha/2)$ .

$$g_{2s} \equiv H_c^{(2s)}\left(\chi - \frac{\alpha}{2}\right) = \sum_{r=0}^{\infty} A_{2r}^{(2s)} \cos 2r\left(\chi - \frac{\alpha}{2}\right) \quad (18)$$

or

$$\begin{aligned} g_{2s+2} &\equiv H_s^{(2s+2)}\left(\chi - \frac{\alpha}{2}\right) \\ &= \sum_{r=2}^{\infty} B_{2r+2}^{(2s+2)} \sin(2r+2)\left(\chi - \frac{\alpha}{2}\right). \end{aligned} \quad (19)$$

$H_c^{(2s)}(\chi - \alpha/2)$  and  $H_s^{(2s+2)}(\chi - \alpha/2)$  possess eigenvalues of  $a_{2s}$  and  $b_{2s+2}$ , respectively.  $A_{2r}^{(2s)}$ ,  $B_{2r+2}^{(2s+2)}$ ,  $a_{2s}$ , and  $b_{2s+2}$  are dependent on  $Q_1$  and  $Q_2$ . For example,

$$\begin{aligned} H_c^{(2)}\left(\chi - \frac{\alpha}{2}\right) &= \frac{1}{4} Q_1 - \frac{1}{12} Q_1 Q_2 - \frac{5}{192} Q_1^3 \\ &+ \frac{13}{1,152} Q_1 Q_2^2 + \dots + \cos 2\left(\chi - \frac{\alpha}{2}\right) \\ &+ \left(-\frac{1}{12} Q_1 - \frac{53}{1,152} Q_1 Q_2 - \frac{43}{13,824} Q_1^3\right. \\ &+ \left.\frac{1879}{184,320} Q_1 Q_2^2 + \dots\right) \cos 4\left(\chi - \frac{\alpha}{2}\right) \\ &+ \left(-\frac{1}{32} Q_2 + \frac{1}{384} Q_1^2 - \frac{1}{1,024} Q_2^2 - \frac{1}{98,304} Q_2^3\right. \\ &+ \left.\frac{97}{92,160} Q_1^2 Q_2 + \dots\right) \cos 6\left(\chi - \frac{\alpha}{2}\right) \\ &+ \left(\frac{11}{5,760} Q_1 Q_2 - \frac{1}{23,040} Q_1^3\right. \\ &+ \left.\frac{373}{460,800} Q_1 Q_2^2 + \dots\right) \cos 8\left(\chi - \frac{\alpha}{2}\right) \\ &+ \left(\frac{1}{3,072} Q_2^2 + \frac{1}{73,728} Q_2^3\right. \\ &- \left.\frac{13}{276,480} Q_1^2 Q_2 + \dots\right) \cos\left(\chi - \frac{\alpha}{2}\right) \\ &+ \left(-\frac{103}{6,451,200} Q_1 Q_2^2 + \dots\right) \cos 12\left(\chi - \frac{\alpha}{2}\right) \\ &+ \left(-\frac{1}{589,824} Q_2^3 + \dots\right) \cos 14\left(\chi - \frac{\alpha}{2}\right) + \dots \end{aligned} \quad (20)$$

and

$$a_2 = 4 + Q_2 + \frac{5}{12} Q_1^2 - \frac{1}{32} Q_2^2 - \frac{1}{1,024} Q_2^3 - \frac{121}{576} Q_1^2 Q_2 + \dots \quad (21)$$

$$\begin{aligned} H_s^{(2)} \left( \chi - \frac{\alpha}{2} \right) &= \sin 2 \left( \chi - \frac{\alpha}{2} \right) \\ &+ \left( -\frac{1}{12} Q_1 + \frac{11}{1,152} Q_1 Q_2 \right. \\ &+ \frac{5}{13,824} Q_1^3 - \frac{151}{184,320} Q_1 Q_2^2 \\ &+ \dots \left. \right) \sin 4 \left( \chi - \frac{\alpha}{2} \right) + \left( -\frac{1}{32} Q_2 \right. \\ &+ \frac{1}{384} Q_1^2 + \frac{1}{1,024} Q_2^2 - \frac{1}{98,304} Q_2^3 \\ &- \frac{11}{30,720} Q_1^2 Q_2 + \dots \left. \right) \sin 6 \left( \chi - \frac{\alpha}{2} \right) \\ &+ \left( \frac{11}{5,760} Q_1 Q_2 - \frac{1}{23,040} Q_1^3 \right. \\ &- \frac{49}{230,400} Q_1 Q_2^2 + \dots \left. \right) \sin 8 \left( \chi - \frac{\alpha}{2} \right) \\ &+ \left( \frac{1}{3,072} Q_2^2 - \frac{1}{73,728} Q_2^3 \right. \\ &- \frac{13}{276,480} Q_1^2 Q_2 + \dots \left. \right) \sin 10 \left( \chi - \frac{\alpha}{2} \right) \\ &+ \left( -\frac{103}{6,451,200} Q_1 Q_2^2 + \dots \right) \sin 12 \left( \chi - \frac{\alpha}{2} \right) \\ &+ \left( -\frac{1}{589,824} Q_2^3 + \dots \right) \sin 14 \left( \chi - \frac{\alpha}{2} \right) + \dots \quad (22) \end{aligned}$$

and

$$b_2 = 4 - Q_2 - \frac{1}{12} Q_1^2 - \frac{1}{32} Q_2^2 + \frac{1}{1,024} Q_2^3 + \frac{7}{576} Q_1^2 Q_2 + \dots \quad (23)$$

The coefficients in Eqs. 20–23 are not normalized.

The transition dipole moment of  $\mathbf{m}_{ia}$  in the molecular system is transformed into  $\mathbf{M}_{ia}$  in the experimental system through a transformation matrix made of  $\mathbf{T}(\psi, \theta, \gamma)$  with Euler angles of  $\psi$ ,  $\theta$ , and  $\gamma$ . The Z component of  $\mathbf{M}_{ia}$ ,  $M_{iaz}(\psi, \theta, \chi)$  may be expanded in terms of associated Legendre polynomials and  $H_c^{(2s)}(\chi - \alpha/2)$  or  $H_s^{(2s+2)}(\chi - \alpha/2)$ , as

follows:

$$\begin{aligned} M_{iaz}(\psi, \theta, \chi) &= \pi \left\{ (\sqrt{2}/3) P_0(\cos \theta) \right. \\ &+ \sqrt{2/5} (\cos^2 \delta_a - \frac{1}{3}) P_2(\cos \theta) \left. \right\} \\ &\sum_{s=0}^{\infty} 2A_0^{(2s)} H_c^{(2s)} \left( \chi - \frac{\alpha}{2} \right) \\ &- \frac{2\pi}{3} \sqrt{\frac{3\pi}{5}} \sin^2 \delta_a P_2^2(\cos \theta) \\ &\cdot \frac{1}{\sqrt{\pi}} \left\{ \cos 2(\psi - \epsilon - \alpha) \sum_{s=0}^{\infty} A_4^{(2s)} H_c^{(2s)} \left( \chi - \frac{\alpha}{2} \right) \right. \\ &+ \sin 2(\psi - \epsilon - \alpha) \sum_{s=0}^{\infty} B_4^{(2s+2)} H_s^{(2s+2)} \left( \chi - \frac{\alpha}{2} \right) \left. \right\} \\ &- \frac{2\pi}{3} \sqrt{\frac{3\pi}{5}} \sin 2\delta_a P_2^1(\cos \theta) \\ &\frac{1}{\sqrt{\pi}} \left\{ \sin(\psi - \epsilon - \alpha) \sum_{s=0}^{\infty} A_2^{(2s)} H_c^{(2s)} \right. \\ &\left( \chi - \frac{\alpha}{2} \right) - \cos(\psi - \epsilon - \alpha) \\ &\left. \sum_{s=0}^{\infty} B_2^{(2s+2)} H_s^{(2s+2)} \left( \chi - \frac{\alpha}{2} \right) \right\} \quad (24) \end{aligned}$$

where  $P_n(\cos \theta)$  and  $P_n^m(\cos \theta)$  are normalized and associated Legendre polynomials, respectively. In Eq. 24, the transformation,  $\phi = 2\chi$ , is made and the expansion coefficients,  $A_0^{(2s)}$ ,  $A_4^{(2s)}$ ,  $B_4^{(2s+2)}$ ,  $A_2^{(2s)}$  and  $B_2^{(2s+2)}$  are normalized.  $M_{iez}^2(\psi, \theta, \chi)$ ,  $M_{ie\chi}^2(\psi, \theta, \chi, \gamma)$ ,  $M_{iez}^2(\psi, \theta, \chi)$  and  $M_{ie\chi}^2(\psi, \theta, \chi, \gamma)$  can be also expanded in the similar way. Now,  $\rho_1(\psi, \theta, \chi, t)$  may be obtained by using Eq. 10 and 11 for the Green function and Eq. 24 for  $M_{iaz}^2(\psi, \theta, \chi)$ .

$$\begin{aligned} \rho_1(\psi, \theta, \chi, t) &= \frac{\pi \sqrt{2}}{3} P_0(\cos \theta) \\ &\cdot \sum_{s=0}^{\infty} 2A_0^{(2s)} H_c^{(2s)} \left( \chi - \frac{\alpha}{2} \right) e^{\lambda_0^{2s} t} \\ &+ \pi \sqrt{\frac{2}{5}} \left( \cos^2 \delta_a - \frac{1}{3} \right) P_2(\cos \theta) \\ &\sum_{s=0}^{\infty} 2A_0^{(2s)} H_c^{(2s)} \left( \chi - \frac{\alpha}{2} \right) e^{\lambda_0^{2s} t} \\ &- \frac{2\pi}{3} \sqrt{\frac{3\pi}{5}} \sin^2 \delta_a P_2^2(\cos \theta) \\ &\frac{1}{\sqrt{\pi}} \left\{ \cos 2(\psi - \epsilon - \alpha) \sum_{s=0}^{\infty} A_4^{(2s)} \right. \end{aligned}$$

$$\begin{aligned}
& \cdot H_c^{(2s)} \left( \chi - \frac{\alpha}{2} \right) e^{\lambda_1^{2s} t} \\
& + \sin 2(\psi - \epsilon - \alpha) \sum_{s=0}^{\infty} B_4^{(2s+2)} H_s^{(2s+2)} \\
& \left( \chi - \frac{\alpha}{2} \right) e^{\lambda_1^{2s+2} t} \left\{ - \frac{2\pi}{3} \sqrt{\frac{3\pi}{5}} \sin 2\delta_a P_2^1(\cos \theta) \right. \\
& \cdot \frac{1}{\sqrt{\pi}} \left[ \sin(\psi - \epsilon - \alpha) \sum_{s=0}^{\infty} \right. \\
& \cdot A_2^{(2s+2)} H_c^{(2s+2)} \left( \chi - \frac{\alpha}{2} \right) e^{\lambda_2^{2s+2} t} \\
& \left. \left. - \cos(\psi - \epsilon - \alpha) \sum_{s=0}^{\infty} B_2^{(2s+2)} H_s^{(2s+2)} \left( \chi - \frac{\alpha}{2} \right) e^{\lambda_2^{2s+2} t} \right] \right\}, \quad (25)
\end{aligned}$$

where

$$\lambda_n^{2s} = -\{k_1 + k_a + n(n+1)D + \frac{1}{4} a_{2s} D_2\} \quad (26)$$

and

$$\nu_n^{2s+2} = -\{k_1 + k_a + n(n+1)D + \frac{1}{4} b_{2s+2} D_2\}. \quad (27)$$

Next,  $\rho_2(\psi\theta\chi t)$  may be obtained in a similar way by using Eq. 13 and 14 for the Green function and  $\rho_1(\psi\theta\chi t)$  as derived above, and also by using the orthogonal relation between  $G_2(\psi_0\theta_0|\psi\theta, t-\tau)$  and  $\rho_1(\psi\theta\chi t)$ .

$$\begin{aligned}
\rho_2(\psi\theta\chi t) &= \frac{\pi\sqrt{2}}{3} P_0(\cos \theta) \\
& \cdot \sum_{s=0}^{\infty} 2A_0^{(2s)} H_c^{(2s)} \left( \chi - \frac{\alpha}{2} \right) \\
& \cdot \frac{k_1(\chi)}{\lambda_0^{2s} - \mu_0} (e^{\lambda_0^{2s} t} - e^{\mu_0 t}) \\
& + \pi \sqrt{\frac{2}{5}} \left( \cos^2 \delta_a - \frac{1}{3} \right) P_2(\cos \theta) \\
& \cdot \sum_{s=0}^{\infty} 2A_0^{(2s)} H_c^{(2s)} \left( \chi - \frac{\alpha}{2} \right) \\
& \cdot \frac{k_1(\chi)}{\lambda_2^{2s} - \mu_2} (e^{\lambda_2^{2s} t} - e^{\mu_2 t}) \\
& - \frac{2\pi}{3} \sqrt{\frac{3\pi}{5}} \sin^2 \delta_a P_2^2(\cos \theta) \\
& \cdot \frac{1}{\sqrt{\pi}} \left[ \sin(\psi - \epsilon - \alpha) \sum_{s=0}^{\infty} A_2^{(2s)} H_c^{(2s)} \left( \chi - \frac{\alpha}{2} \right) \right. \\
& \cdot \frac{k_1(\chi)}{\lambda_2^{2s} - \mu_2} (e^{\lambda_2^{2s} t} - e^{\mu_2 t})
\end{aligned}$$

$$\begin{aligned}
& + \sin 2(\psi - \epsilon - \alpha) \sum_{s=0}^{\infty} B_4^{(2s+2)} H_s^{(2s+2)} \\
& \left( \chi - \frac{\alpha}{2} \right) \frac{k_1(\chi)}{\nu_2^{2s+2} - \mu_2} (e^{\nu_2^{2s+2} t} - e^{\mu_2 t}) \left\{ \right. \\
& - \frac{2\pi}{3} \sqrt{\frac{3\pi}{5}} \sin 2\delta_a P_2^1(\cos \theta) \\
& \cdot \frac{1}{\sqrt{\pi}} \left[ \sin(\psi - \epsilon - \alpha) \sum_{s=0}^{\infty} A_2^{(2s)} H_c^{(2s)} \left( \chi - \frac{\alpha}{2} \right) \right. \\
& \cdot \frac{k_1(\chi)}{\lambda_2^{2s} - \mu_2} (e^{\lambda_2^{2s} t} - e^{\mu_2 t}) \\
& \left. \left. - \cos(\psi - \epsilon - \alpha) \sum_{s=0}^{\infty} B_2^{(2s+2)} H_s^{(2s+2)} \left( \chi - \frac{\alpha}{2} \right) \right. \right. \\
& \left. \left. \frac{k_1(\chi)}{\nu_2^{2s+2} - \mu_2} (e^{\nu_2^{2s+2} t} - e^{\mu_2 t}) \right] \right\} \quad (28)
\end{aligned}$$

where

$$\mu_n = -\{k_2 + n(n+1)D\}. \quad (29)$$

#### FLUORESCENCE DECAY FUNCTION AND ANISOTROPY DECAY

Time dependences of the donor-fluorescence polarized along Z-axis,  $F_{1Z}(t)$ , and X-axis,  $F_{1X}(t)$ , can be obtained from  $\rho_1(\psi\theta\chi t)$  (Chuang and Eisenthal, 1972).

$$\begin{aligned}
F_{1Z}(t) &= 2 \int_0^\pi d\chi \int_0^{2\pi} d\gamma \int_0^{2\pi} d\psi \int_0^\pi \sin\theta d\theta \\
& \cdot M_{1eZ}^2(\psi\theta\chi) \rho_1(\psi\theta\chi t) \quad (30)
\end{aligned}$$

where  $M_{1eZ}(\psi\theta\chi)$  is the Z component of transition dipole moment of donor emission. By using the orthogonal relation between  $\rho_1(\psi\theta\chi t)$  given in Eq. 25 and  $M_{1eZ}^2(\psi\theta\chi)$ ,  $F_{1Z}(t)$  may be obtained as follows:

$$\begin{aligned}
F_{1Z}(t) &= \frac{16}{9} \pi^4 \sum_{s=0}^{\infty} 2\{A_0^{(2s)}\}^2 e^{\lambda_0^{2s} t} \\
& + \frac{16}{5} \pi^4 \left( \cos^2 \delta_a - \frac{1}{3} \right) \left( \cos^2 \delta_e - \frac{1}{3} \right) \\
& \cdot \sum_{s=0}^{\infty} 2\{A_0^{(2s)}\}^2 e^{\lambda_0^{2s} t} \\
& + \frac{8}{15} \pi^4 \sin^2 \delta_a \sin^2 \delta_e \cos 2\epsilon \\
& \cdot \sum_{s=0}^{\infty} [\{A_4^{(2s)}\}^2 e^{\lambda_4^{2s} t} + \{B_4^{(2s+2)}\}^2 e^{\lambda_4^{2s+2} t}] \\
& + \frac{8}{15} \pi^4 \sin 2\delta_a \sin 2\delta_e \cos \epsilon \\
& [\{A_2^{(2s)}\}^2 e^{\lambda_2^{2s} t} + \{B_2^{(2s+2)}\}^2 e^{\lambda_2^{2s+2} t}]. \quad (31)
\end{aligned}$$

On the other hand,

$$\begin{aligned}
 F_{1X}(t) = & 2 \int_0^\pi d\chi \int_0^{2\pi} d\gamma \int_0^{2\pi} d\psi \int_0^\pi \\
 & \sin \theta d\theta M_{\text{ex}}^2(\psi\theta\chi\gamma) \rho_1(\psi\theta\chi t) \\
 = & \frac{16}{9} \pi^4 \sum_{s=0}^\infty 2\{A_0^{(2s)}\}^2 e^{\lambda_0^{2s}t} \\
 & - \frac{8}{5} \pi^4 \left( \cos^2 \delta_a - \frac{1}{3} \right) \\
 & \cdot \left( \cos^2 \delta_e - \frac{1}{3} \right) \sum_{s=0}^\infty 2\{A_0^{(2s)}\}^2 e^{\lambda_2^{2s}t} \\
 & - \frac{4}{15} \pi^4 \sin^2 \delta_a \sin^2 \delta_e \cos 2\epsilon \\
 & \cdot \sum_{s=0}^\infty [\{A_4^{(2s)}\}^2 e^{\lambda_2^{2s}t} + \{B_4^{(2s+2)}\}^2 e^{\lambda_2^{2s+2}t}] \\
 & - \frac{4}{15} \pi^4 \sin 2\delta_a \sin 2\delta_e \cos \epsilon \\
 & \cdot \sum_{s=0}^\infty [\{A_2^{(2s)}\}^2 e^{\lambda_2^{2s}t} + \{B_2^{(2s+2)}\}^2 e^{\lambda_2^{2s+2}t}]. \quad (32)
 \end{aligned}$$

The fluorescence intensities of acceptor under the excitation of donor are obtained from  $\rho_2(\psi\theta\chi t)$ .

$$\begin{aligned}
 F_{2Z}(t) = & \frac{16\pi^4}{9} \sum_{s=0}^\infty A_0^{(2s)} \{2k_a A_0^{(2s)} + k_b A_2^{(2s)} + k_c A_4^{(2s)}\} \\
 & \cdot \frac{1}{\lambda_0^{2s} - \mu_0} (e^{\lambda_0^{2s}t} - e^{\mu_0 t}) \\
 & + \frac{16\pi^4}{5} \left( \cos^2 \delta_a - \frac{1}{3} \right) \left( m_z^2 - \frac{1}{3} \right) \\
 & \cdot \sum_{s=0}^\infty A_0^{(2s)} \{2k_a A_0^{(2s)} + k_b A_2^{(2s)} + k_c A_4^{(2s)}\} \\
 & \cdot \frac{1}{\lambda_2^{2s} - \mu_2} (e^{\lambda_2^{2s}t} - e^{\mu_2 t}) \\
 & + \frac{8\pi^4}{15} \sin^2 \delta_a \{(m_x^2 - m_y^2) \cos 2(\epsilon + \alpha) \\
 & + 2m_x m_y \sin 2(\epsilon + \alpha)\} \\
 & \cdot \sum_{s=0}^\infty A_4^{(2s)} \{2k_a A_0^{(2s)} + k_b A_2^{(2s)} + k_c A_4^{(2s)}\} \\
 & \cdot \frac{1}{\lambda_2^{2s} - \mu_2} (e^{\lambda_2^{2s}t} - e^{\mu_2 t}) \\
 & + \frac{8\pi^4}{5} \sin 2\delta_a m_x m_z \cos(\epsilon + \alpha) \\
 & + m_y m_z \sin(\epsilon + \alpha)\}
 \end{aligned}$$

$$\begin{aligned}
 & \cdot \sum_{s=0}^\infty A_2^{(2s)} \{2k_a A_0^{(2s)} + k_b A_2^{(2s)} \\
 & + k_c A_4^{(2s)}\} \frac{1}{\lambda_2^{2s} - \mu_2} (e^{\lambda_2^{2s}t} - e^{\mu_2 t}) \quad (33)
 \end{aligned}$$

$$\begin{aligned}
 F_{2X}(t) = & \frac{16\pi^4}{9} \sum_{s=0}^\infty A_0^{(2s)} \{2k_a A_0^{(2s)} + k_b A_2^{(2s)} + k_c A_4^{(2s)}\} \\
 & \cdot \frac{1}{\lambda_0^{2s} - \mu_0} (e^{\lambda_0^{2s}t} - e^{\mu_0 t}) \\
 & - \frac{8}{5} \pi^4 \left( \cos^2 \delta_a - \frac{1}{3} \right) \left( m_z^2 - \frac{1}{3} \right) \\
 & \cdot \sum_{s=0}^\infty A_0^{(2s)} \{2k_a A_0^{(2s)} + k_b A_2^{(2s)} + k_c A_4^{(2s)}\} \\
 & \cdot \frac{1}{\lambda_2^{2s} - \mu_0} (e^{\lambda_2^{2s}t} - e^{\mu_0 t}) \\
 & - \frac{4}{15} \pi^4 \sin^2 \delta_a \{(m_x^2 - m_y^2) \cos(\epsilon + \alpha) \\
 & + 2m_x m_z \sin 2(\epsilon + \alpha)\} \\
 & \cdot \sum_{s=0}^\infty A_4^{(2s)} \{2k_a A_0^{(2s)} + k_b A_2^{(2s)} + k_c A_4^{(2s)}\} \\
 & \cdot \frac{1}{\lambda_2^{2s} - \mu_2} (e^{\lambda_2^{2s}t} - e^{\mu_2 t}) \\
 & - \frac{4}{5} \pi^4 \sin 2\delta_a \{m_x m_z \cos(\epsilon + \alpha) \\
 & + m_y m_z \sin(\epsilon + \alpha)\} \\
 & \cdot \sum_{s=0}^\infty A_2^{(2s)} \{2k_a A_0^{(2s)} + k_b A_2^{(2s)} + k_c A_4^{(2s)}\} \\
 & \cdot \frac{1}{\lambda_2^{2s} - \mu_2} (e^{\lambda_2^{2s}t} - e^{\mu_2 t}). \quad (34)
 \end{aligned}$$

In Eqs. 33 and 34,  $m_x$ ,  $m_y$ , and  $m_z$  denote components of transition moment of acceptor emission corresponding to  $m_{2ex}$ ,  $m_{2ey}$ , and  $m_{2ez}$  in Fig. 1. Using these equations, the fluorescence decay functions,  $F_1(t)$  and  $F_2(t)$ , and the anisotropy decays,  $r_1(t)$  and  $r_2(t)$ , are represented as follows:

$$F_1(t) = F_{1Z}(t) + 2F_{1X}(t) = \sum_{s=0}^\infty 2\{A_0^{(2s)}\}^2 e^{\lambda_0^{2s}t} \quad (35)$$

$$\begin{aligned}
 F_2(t) = & F_{2Z}(t) + 2F_{2X}(t) \\
 = & \sum_{s=0}^\infty A_0^{(2s)} \{2k_a A_0^{(2s)} + k_b A_2^{(2s)} + k_c A_4^{(2s)}\} \\
 & \cdot \frac{1}{\lambda_2^{2s} - \mu_0} (e^{\lambda_2^{2s}t} - e^{\mu_0 t}) \quad (36)
 \end{aligned}$$

$$\begin{aligned}
r_1(t) &= \frac{F_{1z}(t) - F_{1x}(t)}{F_{1z}(t) + 2F_{1x}(t)} \\
&= \frac{1}{F_1(t)} \left[ \frac{1}{10} (3 \cos^2 \delta_a - 1) \right. \\
&\quad (3 \cos^2 \delta_e - 1) \sum_{s=0}^{\infty} 2\{A_0^{(2s)}\}^2 e^{\lambda_0^{2s} t} \\
&\quad + \frac{3}{20} \sin^2 \delta_a \sin^2 \delta_e \cos 2\epsilon \sum_{s=0}^{\infty} \\
&\quad (\{A_4^{(2s)}\}^2 e^{\lambda_4^{2s} t} + \{B_4^{(2s+2)}\}^2 e^{\nu_4^{2s+2} t}) \\
&\quad + \frac{3}{20} \sin 2\delta_a \sin 2\delta_e \cos \epsilon \sum_{s=0}^{\infty} \\
&\quad \left. (\{A_2^{(2s)}\}^2 e^{\lambda_2^{2s} t} + \{B_2^{(2s+2)}\}^2 e^{\nu_2^{2s+2} t}) \right] \quad (37)
\end{aligned}$$

$$\begin{aligned}
r_2(t) &= \frac{F_{2z}(t) - F_{2x}(t)}{F_{2z}(t) + F_{2x}(t)} \\
&= \frac{1}{F_2(t)} \left[ \frac{1}{10} (3 \cos^2 \delta_a - 1)(3m_z^2 - 1) \sum_{s=0}^{\infty} A_0^{(2s)} \right. \\
&\quad + \frac{3}{20} \sin^2 \delta_a \{(m_x^2 - m_y^2) \cos 2(\epsilon + \alpha) \\
&\quad + 2m_x m_y \sin 2(\epsilon + \alpha)\} \sum_{s=0}^{\infty} A_4^{(2s)} \\
&\quad + \frac{9}{20} \sin 2\delta_a \{m_x m_z \cos(\epsilon + \alpha) \\
&\quad + m_y m_z \sin(\epsilon + \alpha)\} \sum_{s=0}^{\infty} A_2^{(2s)} \left. \right] \\
&\quad \{2k_a A_0^{(2s)} + k_b A_2^{(2s)} \\
&\quad + k_c A_4^{(2s)}\} \frac{1}{\lambda_2^{2s} - \mu_2} (e^{\lambda_0^{2s} t} - e^{\mu_2 t}). \quad (38)
\end{aligned}$$

#### FLUORESCENCE INTENSITY AND ANISOTROPY UNDER STEADY-STATE EXCITATION

The expressions for the fluorescence quantum yield ( $q$ ) and the anisotropy ( $r$ ) of the energy donor and acceptor under the excitation of the donor with constant light source are obtained from Eqs. 31–34 by integrating  $F_{1z}(t)$ ,  $F_{1x}(t)$ ,  $F_{2z}(t)$  and  $F_{2x}(t)$  over  $t$  from  $t=0$  to  $t=\infty$ .

$$q_1 = -k_{1f} \sum_{s=0}^{\infty} \frac{2\{A_0^{(2s)}\}^2}{\lambda_0^{2s}} \quad (39)$$

$$q_2 = k_{2f} \sum_{s=0}^{\infty} \frac{A_0^{(2s)} \{2k_a A_0^{(2s)} + k_b A_2^{(2s)} + k_c A_4^{(2s)}\}}{\lambda_0^{2s} \mu_0} \quad (40)$$

$$\begin{aligned}
r_1 &= \frac{-1}{q_1} \left[ \frac{1}{10} (3 \cos^2 \delta_a - 1) \right. \\
&\quad (3 \cos^2 \delta_e - 1) \sum_{s=0}^{\infty} \frac{2\{A_0^{(2s)}\}^2}{\lambda_2^{2s}} \\
&\quad + \frac{3}{20} \sin^2 \delta_a \sin^2 \delta_e \cos 2\epsilon \sum_{s=0}^{\infty} \\
&\quad \cdot \left( \frac{\{A_4^{(2s)}\}^2}{\lambda_2^{2s}} + \frac{\{B_4^{(2s+2)}\}^2}{\nu_2^{2s+2}} \right) \\
&\quad + \frac{3}{20} \sin 2\delta_a \sin 2\delta_e \cos \epsilon \sum_{s=0}^{\infty} \\
&\quad \cdot \left. \left( \frac{\{A_2^{(2s)}\}^2}{\lambda_2^{2s}} + \frac{\{B_2^{(2s+2)}\}^2}{\nu_2^{2s+2}} \right) \right] \quad (41)
\end{aligned}$$

$$\begin{aligned}
r_2 &= \frac{1}{q_2} \left[ \frac{1}{10} (3 \cos^2 \delta_a - 1) \right. \\
&\quad \cdot (3m_z^2 - 1) \sum_{s=0}^{\infty} A_0^{(2s)} \\
&\quad + \frac{3}{20} \sin^2 \delta_a \{(m_x^2 - m_y^2) \cos 2(\epsilon + \alpha) \\
&\quad + 2m_x m_y \sin 2(\epsilon + \alpha)\} \sum_{s=0}^{\infty} A_4^{(2s)} \\
&\quad + \frac{9}{20} \sin 2\delta_a \{m_x m_z \cos(\epsilon + \alpha) \\
&\quad + m_y m_z \sin(\epsilon + \alpha)\} \sum_{s=0}^{\infty} A_2^{(2s)} \left. \right] \\
&\quad \cdot \frac{\{2k_a A_0^{(2s)} + k_b A_2^{(2s)} + k_c A_4^{(2s)}\}}{\lambda_2^{2s} - \mu_2}. \quad (42)
\end{aligned}$$

In Eqs. 39 and 40  $k_{1f}$  and  $k_{2f}$  represent radiative transition probabilities of donor and acceptor, respectively.

#### LIMITING CASES AT VERY FAST AND SLOW INTERNAL ROTATION OF ENERGY DONOR

The behavior of the decay function and anisotropy decay was examined when  $D_R \rightarrow \infty$  and  $D_R \rightarrow 0$ . At large values of  $D_R$ , both  $Q_1$  and  $Q_2$  become negligibly small. In this case,  $A_0^{(0)} = 1/\sqrt{2}$ ,  $A_0^{(2s)} = 0$ ,  $A_2^{(2s)} = B_2^{(2s+2)} = \delta_{sr}$  and  $a_{2s} = 4s^2$ ,  $b_{2s+2} = 4(s+1)^2$ . Then

$$F_1(t) \simeq e^{-(k_1 + k_a)t} \quad (43)$$

and

$$F_2(t) \simeq \frac{k_a}{k_2 - k_1 - k_a} (e^{-(k_1 + k_a)t} - e^{-k_2 t}). \quad (44)$$

Since the averaged value of  $k_i(\chi)$  over  $\chi$  from 0 to  $\pi$  ( $\phi = 0$ )

to  $2\pi$ ) is  $2\pi k_a$ ,  $F_1(t)$  and  $F_2(t)$  decay with the averaged energy transfer rate, which is essentially similar to the case of energy transfer in solution where both energy donor and acceptor are freely mobile during the lifetime of the donor.

Also, with appropriate substitutions into Eqs. 31–34, and 37–38

$$r_1(t) \approx \frac{1}{10} (3 \cos^2 \delta_a - 1)(3 \cos^2 \delta_e - 1)e^{-6Dt} + \frac{3}{10} \sin^2 \delta_a \sin^2 \delta_e \cos \epsilon e^{-(6D+4D_1)t} + \frac{3}{10} \sin 2\delta_a \sin 2\delta_e \cos \epsilon e^{-(6D+D_1)t} \quad (45)$$

and

$$r_2(t) \approx \frac{1}{10} (3 \cos^2 \delta_a - 1)(3m_z^2 - 1)e^{-6Dt}. \quad (46)$$

Eq. 45 for  $r_1(t)$  is the same as the expression obtained by Gotlib and Wahl (1963) for internal rotation which is very fast compared with the energy transfer probability, i.e.,  $D_1 \gg k_b$  and  $D_1 \gg k_c$ .

Next we examine the behavior of  $F_1(t)$  at  $D_1 = 0$ . When  $\mathbf{m}_{1a}$  and  $\mathbf{m}_{1e}$  are fixed and distributed uniformly around the  $z$ -axis, it is convenient to approach the problem with an alternative method. Since a donor interacts only with one acceptor molecule within the entity of the macromolecule, the decay function,  $F_{1i}(t)$ , may be represented as follows (Mataga and Kubota, 1970):

$$F_{1i}(t) = e^{-(k_1 + k_i(\phi_i))t}. \quad (47)$$

The decay function corresponding to the observed one can be obtained by averaging  $F_{1i}(t)$  over a macroscopic ensemble of  $\phi_i$ .

$$\overline{F_1(t)} = \frac{1}{2\pi} e^{-(k_1 + k_a)t} \int_0^{2\pi} d\phi e^{-[k_b \cos(\phi - \alpha) + k_c \cos 2(\phi - \alpha)]t} = e^{-(k_1 + k_a)t} \left\{ I_0(k_b t) I_0(k_c t) + 2 \sum_{n=1}^{\infty} \sum_{r=0}^{[n-1/2]} \left( -\frac{k_c t}{2} \right)^n \frac{I_2(n-2r)(k_b t)}{(n-r)! r!} \right\} \quad (48)$$

where  $[n-1/2]$  means the maximum integer equal or less than  $1/2(n-1)$ .  $I_p(x)$  represents a modified Bessel function of the first kind with order  $p$ ,

$$I_p(x) = \left( \frac{x}{2} \right)^p \sum_{n=0}^{\infty} \frac{(x/2)^{2n}}{n!(n+p)!}. \quad (49)$$

When  $k_b t \approx 0$  and  $k_c t \approx 0$ ,

$$\overline{F_1(t)} = e^{-(k_1 + k_a)t + (1/4)(k_b^2 + k_c^2)t^2} \quad (50)$$

and as  $t \rightarrow \infty$

$$\overline{F_1(t)} = \frac{1}{2\pi} e^{-(k_1 + k_a - k_b - k_c)t - \log t \sqrt{k_b k_c}} \quad (51)$$

From Eqs. 50 and 51, it is evident that the decay function of the donor should be non-exponential when the internal rotation is very slow and the apparent decay constant is smaller in the longer time range than in the shorter time range. In this situation, a part of the ensemble of  $\mathbf{m}_{1ei}$ ,  $\{\mathbf{m}_{1ei}\}$ , could have angles,  $\delta$ , between those of  $\mathbf{m}_{1e}$  and  $\mathbf{m}_{2a}$  so that  $k_i(\phi_i)$  would be less than  $k_a$ . Therefore, it is reasonable to see the appearance of the component with a decay rate less than  $k_1 + k_a$ .

## NUMERICAL ANALYSIS OF THE EFFECT OF INTERNAL ROTATION

Characteristic values and expansion coefficients of Hill's functions are dependent on  $Q_1$  and  $Q_2$  as shown in Eqs. 20–23. Since these are complex polynomials of  $Q_1$  and  $Q_2$ , it may be difficult to obtain  $D_1$  and other parameters concerning mutual orientations of donor and acceptor from observed decay functions of  $F_1(t)$  and  $F_2(t)$  or observed anisotropy decays of  $r_1(t)$  and  $r_2(t)$ . These parameters may be obtained with a computer by the following best-fitting procedure.

$A_{2r}^{(2s)}$  of  $H_s^{(2s)}(\chi - \alpha/2)$  in Eq. 18 are determined by solving the system of simultaneous linear equations with an infinite number of unknowns.

$$\begin{aligned} -a A_0 + Q_1 A_2 + Q_2 A_4 &= 0 \\ Q_1 A_0 + (4-a) A_2 + Q_1 A_4 + Q_2 A_6 &= 0 \\ &\vdots \\ Q_2 A_{2(r-2)} + Q_1 A_{2(r-1)} + (4r^2 - a) A_{2r} + Q_1 A_{2(r+1)} &+ Q_2 A_{2(r+2)} = 0 \end{aligned} \quad (r \geq 2) \quad (52)$$

In a similar way  $B_{2r+2}^{(2s+2)}$  of  $H_s^{(2s+2)}(\chi - \alpha/2)$  in Eq. 19 are determined by solving the following linear simultaneous equations.

$$\left. \begin{aligned} (4-b) B_2 + Q_1 B_4 + Q_2 B_6 &= 0 \\ Q_1 B_2 + (16-b) B_4 + Q_1 B_6 + Q_2 B_8 &= 0 \\ Q_2 B_{2(r-1)} + Q_1 B_{2r} + \{4(r+1)^2 - b\} B_{2(r+1)} &+ Q_1 B_{2(r+2)} + Q_2 B_{2(r+2)} = 0 \end{aligned} \right\} \quad (r \geq 2) \quad (53)$$

In order to obtain definite solutions of  $A_{2r}$  and  $B_{2r+2}$  the characteristic values of  $a$  and  $b$  must satisfy the secular equations of Eqs. 54 and 55, respectively.



$$\begin{vmatrix} -a & Q_1 & Q_2 & 0 & 0 & 0 & \dots \\ Q_1 & (4-a) & Q_1 & Q_2 & 0 & 0 & \dots \\ Q_2 & Q_1 & (16-a) & Q_1 & Q_2 & 0 & \dots \\ \dots & & & & & & \\ \dots & & Q_2 & Q_1 & (4r^2-a) & Q_1 & Q_2 \dots \end{vmatrix} = 0 \quad (54)$$

$$\begin{vmatrix} (4-b) & Q_1 & Q_2 & 0 & 0 & 0 & \dots \\ Q_1 & (16-b) & Q_1 & Q_2 & 0 & 0 & \dots \\ \dots & & & & & & \\ \dots & & Q_2 & Q_1 & \{4(r+1)^2-b\} & Q_1 & Q_2 \dots \end{vmatrix} = 0 \quad (55)$$

Eqs. 54 and 55 can be expanded into an infinite power series of  $a$  and  $b$ . If we approximate the polynomials of infinite order with polynomials of order  $n$  with  $n$  sufficiently large, we obtain  $n$  real roots of  $a$  and  $b$ . The roots are  $a_{2s}$  and  $b_{2s+2}$  ( $s = 0$  to  $n-1$ ) and corresponding to these,  $A_{2s}^{(2s)}$  and  $B_{2s+2}^{(2s+2)}$  ( $r = 0$  to  $n-1$ ) may be determined. Then according to Eqs. 35–38  $F_1(t)$ ,  $F_2(t)$ ,  $r_1(t)$  and  $r_2(t)$  can be calculated for appropriate values of  $Q_1$  and  $Q_2$ .  $Q_1$  and  $Q_2$  may be determined so that the calculated decay functions and anisotropy decays fit well the observed ones.

### MODEL SYSTEM

Numerical calculation was made in a simplified case of geometrical arrangement, where both of  $\mathbf{R}$  and  $\mathbf{m}_{2a}$  were located along the  $y$ -axis, namely,  $R_y = m_{2ay} = 1$  and  $R_x = R_z = m_{2ax} = m_{2az} = 0$ . In this case  $k_i(\phi)$  is expressed as

$$k_i(\phi) = k_a(1 - \cos 2\phi) \quad (56)$$

where  $2\pi k_a$  is an averaged value of  $k_i(\phi)$  over  $\phi$ , and represented as

$$k_a = 2k_1 \sin^2 \delta_c \left( \frac{R_0}{R} \right)^6. \quad (57)$$

In the present model,  $k_b = 0$ ,  $k_a = k_c$  and  $\alpha = \pi/2$ . then,  $Q_1 = 0$ ,  $Q_2 = 4Q$ , and Eq. 15 becomes

$$\frac{d^2 g_s}{d\phi^2} + (p_s + 2Q \cos 2\phi) g_s = 0 \quad (58)$$

where  $\phi = 2\chi$  and  $p_s = \frac{1}{4} a_s$  or  $\frac{1}{4} b_s \cdot g_s$ , which satisfies Eq. 58, is the Mathieu function (McLachlan, 1949), and  $H_c^{(2s)}(\chi - \alpha/2)$ , and  $H_s^{(2s+2)}(\chi - \alpha/2)$  in Eqs. 18 and 19 convert into Mathieu functions.

The parameters used for the calculation are listed in Table I. The value of  $k_a$  was changed from  $0.0173 \text{ ns}^{-1}$  to  $2.28 \text{ ns}^{-1}$  as  $\delta_a$  was varied from  $5^\circ$  to  $90^\circ$  (see Fig. 2). In Fig. 2, the values of  $D_t$  are shown as  $Q$  changes from 0.01 to 50 at each value of  $\delta_a$ . In Figs. 3 and 4,  $F_1(t)$  (A) and  $F_2(t)$  (B) are shown at  $\delta_a = 30^\circ$  and  $90^\circ$ , respectively.

TABLE I  
VALUES OF PARAMETERS USED FOR THE NUMERICAL CALCULATION

$k_1$	$k_2$	$\delta_c$	$R_0/R$	$D$	$m_x^2$	$m_y^2$	$m_z^2$
$\text{ns}^{-1}$	$\text{ns}^{-1}$			$\text{ns}^{-1}$			
0.1	0.5	equal to $\delta_a$	1.5	0.1	0	1.0	0

When  $Q < 0.5$ , where  $D_t > k_a$ ,  $F_1(t)$  is a nearly single exponential with a time constant of  $k_1 + k_a$ . However, as  $Q$  becomes larger,  $F_1(t)$  decays with the non-exponential function. Deviation of  $F_1(t)$  from the exponential function is more pronounced at shorter time range. The time constant at longer time range approaches  $k_1$  as  $Q \rightarrow \infty$  with  $D_t \rightarrow 0$ .

A similar behavior may also be observed in the case of  $F_2(t)$ . When  $Q < 0.5$ ,  $D_t \geq k_a$ ,  $F_2(t)$  is close to that given in Eq. 44. Deviation of  $F_2(t)$  from Eq. 44 may be also observed at shorter time range. In Figs. 5 and 6,  $r_1(t)$  (A) and  $r_2(t)$  (B) are shown with  $\delta_a = 30^\circ$  and  $90^\circ$ , respectively. The effect of internal rotation on  $r_1(t)$  becomes apparent when  $D_t$  is much larger than  $D$ . In this case, changes in  $r_1(t)$  are apparently similar to the case in the absence of energy transfer. As internal rotation becomes slower ( $D_t \rightarrow 0$ ),  $r_1(t)$  approaches single exponential function with a time constant of  $6D$ . On the other hand, the behavior of  $r_2(t)$  strongly depends on  $\delta_a$ . At  $\delta_a < 55^\circ$ ,  $3 \cos^2 \delta_a - 1 < 0$  and  $r_2(t)$  becomes negative. At  $\delta_a = 30^\circ$ ,  $r_2(t)$  increased with  $t$  to zero. At  $\delta_a = 90^\circ$ ,  $r_2(t)$  decreases from positive maximum value to zero. It should be noted that the

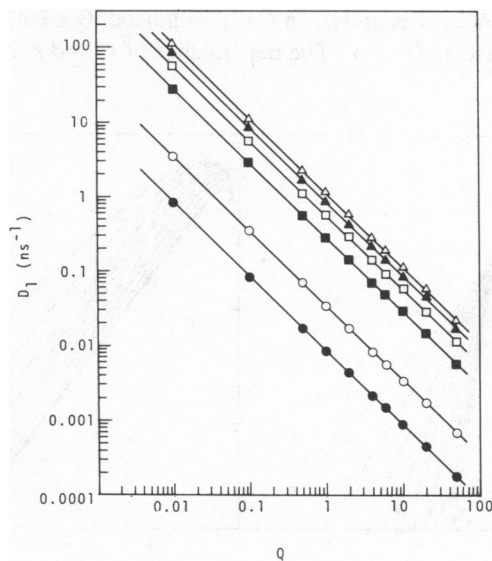


FIGURE 2 Dependence of  $D_t$  on  $Q$ . In the present model  $Q = k_a/2D_t$ , and  $\delta_a$  was assumed to be equal to  $\delta_c$ . The values of  $\delta_a$  are  $5^\circ$  in  $\bullet$ ,  $10^\circ$  in  $\circ$ ,  $30^\circ$  in  $\blacksquare$ ,  $45^\circ$  in  $\square$ ,  $60^\circ$  in  $\blacktriangle$ , and  $90^\circ$  in  $\triangle$ . The values of  $k_a$  corresponding to  $\delta_a = 5^\circ, 10^\circ, 30^\circ, 45^\circ, 60^\circ$ , and  $90^\circ$  are (in  $\text{ns}^{-1}$ ) 0.0173, 0.0687, 0.570, 1.14, 1.71, and 2.28, respectively. The parameters used for numerical calculations are listed in Table I.

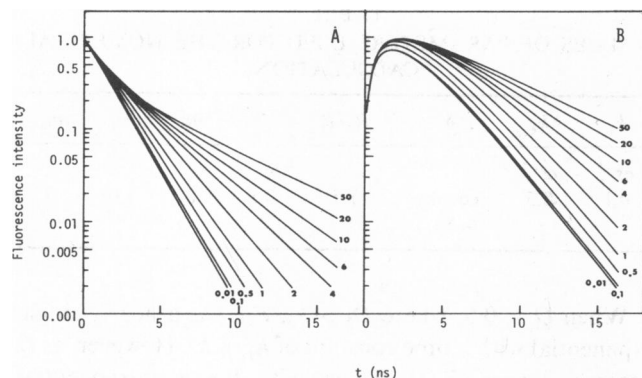


FIGURE 3 Effect of internal rotation on the fluorescence decay functions at  $\delta_a = 30^\circ$ . Fluorescence decay functions of donor (A) and acceptor (B) were calculated as a function of  $Q$ . The curves are labeled with the values of  $Q$ . The parameters used for the calculation are listed in Table I.

behavior of  $r_2(t)$  at shorter time range is dependent on  $Q$ . Namely, when  $D_r$  is considerably larger than  $k_a$ , i.e.  $Q = 0.01$  or  $0.1$ ,  $r_2(t)$  decays exponentially with a time constant of  $6D$ . However, in the range of  $Q$  from  $0.5$  to  $2$ ,  $r_2(t)$  decays with downward concave form at shorter time range, where  $r_2(t)$  deviates from  $\exp(-6Dt)$ . Contrary to this, in the range of  $Q > 4$ ,  $r_2(t)$  decays with upward concave form at shorter time range. The maximum value of  $r_2(t)$  at zero time seemed to decrease a little as  $Q$  increases.

Relative quantum yield and polarization anisotropy of donor and acceptor under steady-state excitation were also calculated by Eqs. 39–42.  $q_1$  and  $q_2$  are shown in Fig. 7A and B, respectively. At  $\delta_a = 5^\circ$  and  $10^\circ$ ,  $q_1$  and  $q_2$  changed a little as a function of  $Q$ . As  $\delta_a$  becomes larger  $q_1$  decreases due to increasing  $k_a$  while  $q_2$  increases, and further the dependences of  $q_1$  and  $q_2$  on  $Q$  are enhanced. Both of  $q_1$  and  $q_2$  increase as  $Q \rightarrow \infty$ . The dependence of  $r_1$  and  $r_2$  on  $\delta_a$  is

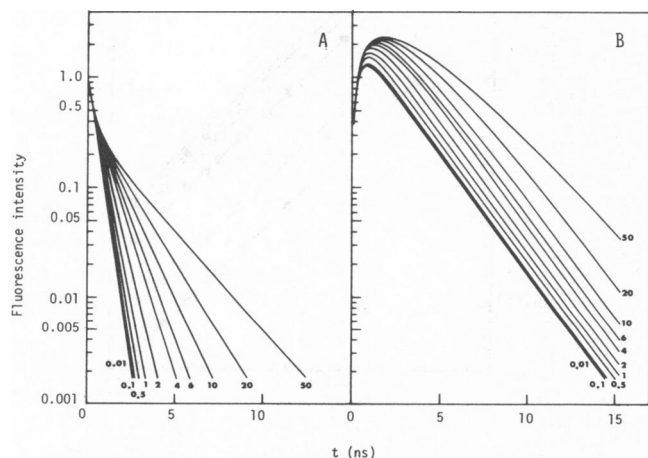


FIGURE 4 Effect of internal rotation on the fluorescence decay functions at  $\delta_a = 90^\circ$ . Fluorescence decay functions of donor (A) and acceptor (B) were calculated as a function of  $Q$ . The curves are labeled with the values of  $Q$ . The parameters used for the calculation are listed in Table I.

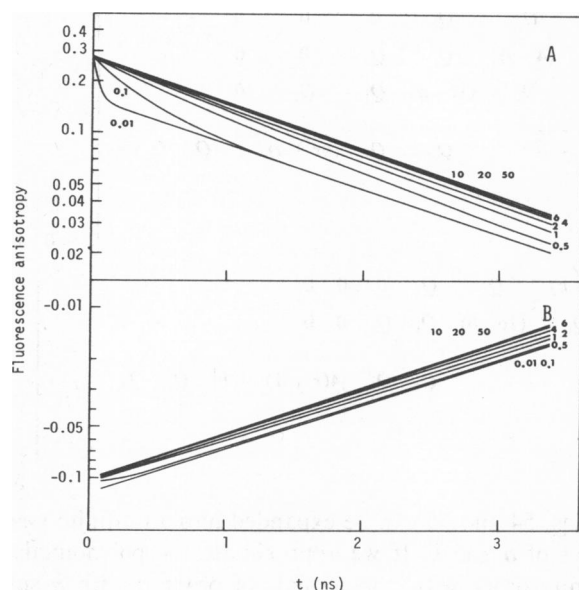


FIGURE 5 Effect of internal rotation on the fluorescence anisotropy decays at  $\delta_a = 30^\circ$ . The anisotropy decays of donor (A) and acceptor (B) were calculated as a function of  $Q$ . The curves are labeled with the values of  $Q$ . The parameters used for the calculation are listed in Table I.

not so straightforward as that of  $q_1$  and  $q_2$ , probably because the angular part of each term originated from the pre-exponential factor. The slight dependence of  $r_1$  and  $r_2$  on  $Q$  at  $\delta_a = 5^\circ$  and  $10^\circ$ , seems reasonable, considering the small effect of internal rotation on  $k_i(\phi)$ . It is significant that both  $r_1$  and  $r_2$ , as functions of  $Q$ , exhibit a maximum.

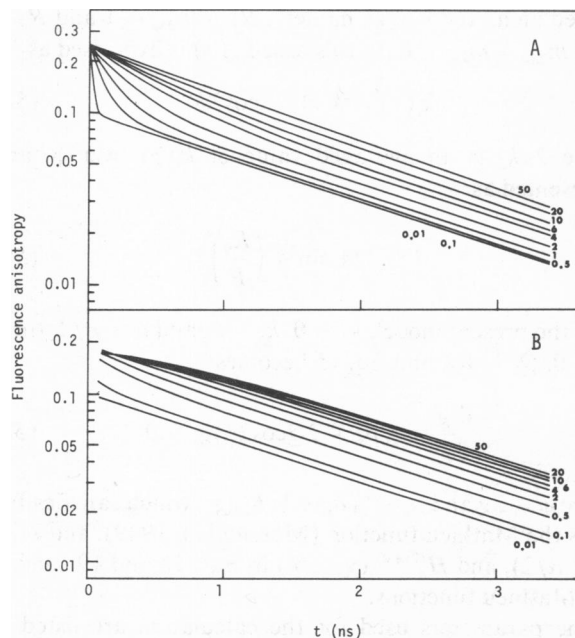


FIGURE 6 Effect of internal rotation on the fluorescence anisotropy decay at  $\delta_a = 90^\circ$ . The anisotropy decays of donor (A) and acceptor (B) were calculated as a function of  $Q$ . The curves are labeled with the values of  $Q$ . The parameters used for the calculation are listed in Table I.

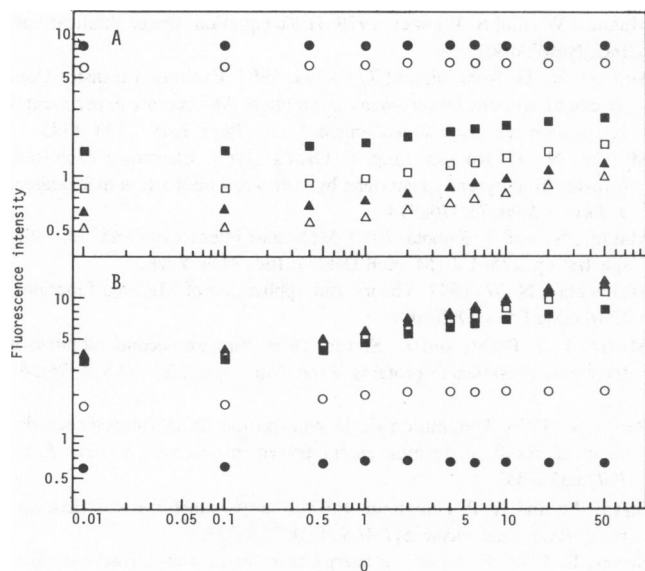


FIGURE 7 Effect of internal rotation on the fluorescence intensity under steady-state excitation. The fluorescence intensities of donor (A) and acceptor (B) under steady-state excitation were calculated for various values of  $Q$ . The values of  $\delta_i$  are  $5^\circ$  in  $\bullet$ ,  $10^\circ$  in  $\circ$ ,  $30^\circ$  in  $\blacksquare$ ,  $45^\circ$  in  $\square$ ,  $60^\circ$  in  $\blacktriangle$ , and  $90^\circ$  in  $\triangle$ . The parameters used for the calculation are listed in Table I.

## DISCUSSION

The effect of internal rotation on the fluorescence decay function, anisotropy decay, relative quantum yield, and the anisotropy under steady-state excitation were investigated under conditions of intramolecular energy transfer interaction. A large number of proteins possess aromatic cofactors, including hemes, which are considered to be fixed in the protein moiety and are potential acceptors of excitation energy from aromatic amino acid residues. In these systems rotational freedom of the aromatic amino acid residues in proteins may be analyzed by the present method.

In the absence of the energy-transfer interaction, the fluorescence decay function of an energy donor is a single exponential. The effect of internal rotation cannot be observed in the decay function but only by fluorescence anisotropy measurements. However, the energy transfer interaction could induce non-exponential decay at  $D_t < k_a$ , owing to the dependence of the transfer probability on the angle of internal rotation. The appearance of a non-exponential function in the present case is somewhat similar to the case of intermolecular energy transfer (Yguerabide et al., 1964; Mataga et al., 1967, 1969) and excimer formation (Vanderkooi and Callis, 1974) in viscous solution. Such a non-exponential behavior of the fluorescence decay could not arise in the case of the energy transfer interaction between a fixed donor and acceptor (without internal rotation) at a definite distance but seems to be quite general when the quenching probability of a fluorophore depends on the internal rotation angles in the

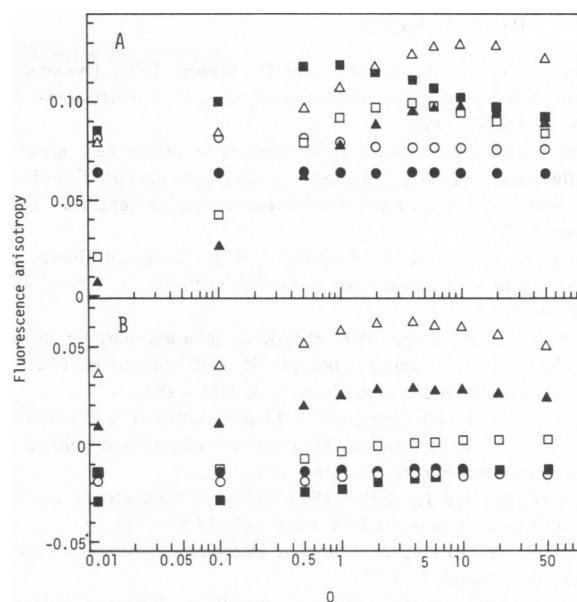


FIGURE 8 Effect of internal rotation on the anisotropy under steady-state excitation. The anisotropies of donor (A) and acceptor (B) under steady-state excitation were calculated at various values of  $Q$ . The values of  $\delta_i$  are  $5^\circ$  in  $\bullet$ ,  $10^\circ$  in  $\circ$ ,  $30^\circ$  in  $\blacksquare$ ,  $45^\circ$  in  $\square$ ,  $60^\circ$  in  $\blacktriangle$ , and  $90^\circ$  in  $\triangle$ . The parameters used for the calculation are listed in Table I.

presence of intermolecular interaction. In fact Wahl (1975a) considered a theoretical model where chromophores perform a local Brownian motion about a fixed axis on macromolecules, and their fluorescence is quenched completely at certain angles of the rotation. The fluorescence decay was predicted to be non-exponential in a short time range. In this case the quenching probability is proportional to the rotational diffusion constant.

Considerable work has been carried out on the determination of distances between the fluorophores bound to macromolecule through the analysis of energy-transfer interaction (Stryer, 1978). Dale et al. (1979) pointed out that in some cases deviation of the orientation factor from assumed averaged values of  $2/3$  or  $0.476$  could be pose serious problems. The effect of the freedom of internal rotation of the energy donor or acceptor on the orientation factor has been systematically investigated. However, the time dependence of the decay function or anisotropy decay have never been examined.

Considering the importance of internal motion of proteins (Gurd and Rothgeb, 1979), the present method of analyzing the effect of internal rotation of a fluorophore on energy transfer interaction could provide an useful tool for the investigation of molecular dynamics of protein structure.

Received for publication 24 June 1981 and in revised form 29 December 1981.

## REFERENCES

- Belford, G. G., R. L. Belford, and G. Weber. 1972. Dynamics of fluorescence polarization in macromolecules. *Proc. Natl. Acad. Sci., U.S.A.* 69:1392-1393.
- Brochon, J.-C., and Ph. Wahl. 1972. Mesures des déclin de l'anisotropie de fluorescence de la  $\gamma$ -globuline et de ses fragments Fab, Fc et F(ab)<sub>2</sub> marqués avec le 1-sulfonyl-5-diméthyl-aminonaphthalène. *Eur. J. Biochem.* 25:20-32.
- Chuang, T. J., and K. B. Eisenthal. 1972. Theory of fluorescence depolarization by anisotropic rotational diffusion. *J. Chem. Phys.* 57:5094-5097.
- Dale, R. E., and J. Eisinger. 1975. Polarized excitation energy transfer. In *Biochemical Fluorescence: Concepts*. R. F. Chen and H. Edelhoch, editors. Marcel Dekker, Inc., New York, 1:115-284.
- Dale, R. E., W. E. Blumberg, and J. Eisinger. 1979. The Orientational freedom of molecular probes. The orientation factor in intramolecular energy transfer. *Biophys. J.* 26:161-193.
- Ehrenberg, M., and R. Rigler. 1972. Polarized fluorescence and rotational Brownian motion. *Chem. Phys. Lett.* 14:539-544.
- Förster, Th. 1948. Zwischenmolekulare Energiewanderung und Fluoreszenz. *Ann. Physik.* 2:55-75.
- Förster, Th. 1951. Fluoreszenz organischer Verbindungen. Vandenhoeck and Ruprecht. Göttingen. 83-86, 172-180, 226-227.
- Gottlieb, Yu. Y., and Ph. Wahl. 1963. Étude théorique de la polarisation de fluorescence des macromolécules portant un groupe émetteur mobile autour d'un axe de rotation. *J. Chim. Phys.* 60:849-856.
- Gurd, F. R. N., and T. M. Rothgeb. 1979. Motions in proteins. *Adv. Protein Chem.* 33:73-165.
- Haugland, R. P., J. Yguerabide, and L. Stryer. 1969. Dependence of the kinetics of singlet-singlet energy transfer on spectral overlap. *Proc. Natl. Acad. Sci. U.S.A.* 63:23-30.
- Jabłoński, A. 1961. Über die Abklingungsvorgänge polarisierter Photolumineszenz. *Z. Naturforsch.* 16a: 1-4.
- Knopp, J. A., and G. Weber. 1969. Fluorescence polarization of pyrene-butyric-bovine serum albumin and pyrene-butyric-human macroglobulin conjugates. *J. Biol. Chem.* 244:6309-6315.
- Lakowicz, J. R., and H. Cherek. 1980. Dipolar relaxation in proteins in the nanosecond timescale observed by wavelength-resolved phase fluorometry of tryptophan fluorescence. *J. Biol. Chem.* 255:831-834.
- Lakowicz, J. R., and G. Weber. 1980. Nanosecond segmental mobilities of tryptophan residues in proteins observed by lifetime-resolved fluorescence. *Biophys. J.* 32:591-601.
- Latt, S. A., H. T. Cheung, and E. R. Blout. 1965. Energy transfer. A system with relatively fixed donor-acceptor separation. *J. Am. Chem. Soc.* 87:995-1003.
- Lombardi, J. R., and G. A. Dafforn. 1966. Anisotropic rotational relaxation in rigid media by polarized photoselection. *J. Chem. Phys.* 44:3882-3887.
- Magnus, W., and S. Winkler. 1979. Hill's equation. Dover Publications, Inc., New York.
- Mataga, N., H. Kobashi, and T. Okada. 1967. Excitation transfer from pyrene to perylene by very weak interaction. An accurate experimental verification of Förster's mechanism. *Chem. Phys. Lett.* 1:133-134.
- Mataga, N., H. Kobashi, and T. Okada. 1969. Electronic excitation transfer from pyrene to perylene by very weak interaction mechanism. *J. Phys. Chem.* 73:370-374.
- Mataga, N., and T. Kubota. 1970. Molecular interactions and electronic spectra. pp. 175-180. Marcell Dekker, Inc., New York.
- McLachlan, N. W. 1947. Theory and application of Mathieu functions. Clarendon Press. Oxford.
- Munro, I., I. Pecht, and L. Stryer. 1979. Subnanosecond motions of tryptophan residues in proteins. *Proc. Natl. Acad. Sci. U.S.A.* 76:56-60.
- Perrin, F. 1936. Diminution de la polarisation de la fluorescence des solutions résultant du mouvement brownien de rotation. *Acta Phys. Pol.* 5:335-347.
- Stryer, L., and R. P. Haugland. 1967. Energy transfer: a spectroscopic ruler. *Proc. Natl. Acad. Sci. U.S.A.* 58:719-726.
- Stryer, L. 1978. Fluorescence energy transfer as a spectroscopic ruler. *Ann. Rev. Biochem.* 47:819-846.
- Tanaka, F., and N. Mataga. 1979. Theory of time-dependent photoselection in interacting fixed systems. *Photochem. Photobiol.* 29:1091-1097.
- Tao, T. 1969. Time-dependent fluorescence depolarization and Brownian rotational diffusion coefficients of macromolecules. *Biopolymers.* 8:609-632.
- Vanderkooi, J. M., and J. B. Callis. 1974. Pyrene. A probe of lateral diffusion in the hydrophobic region of membranes. *Biochemistry.* 13:4000-4006.
- Wahl, Ph., and G. Weber. 1967. Fluorescence depolarization of rabbit gamma globulin conjugates. *J. Mol. Biol.* 30:371-382.
- Wahl, Ph. 1975a. Theoretical determination of decay, quantum yield and anisotropy of chromophores attached to macromolecules and performing a local Brownian motion. *Chem. Phys.* 7:220-228.
- Wahl, Ph. 1975b. Decay of fluorescence anisotropy. In *Biochemical Fluorescence: Concepts*. R. F. Chen and H. Edelhoch, editors. Marcel Dekker, Inc., New York. Vol. I:1-41.
- Weber, G. 1952. Polarization of the fluorescence of macromolecules. *Biochem. J.* 51:145-167.
- Weber, G. 1971. Theory of fluorescence depolarization by anisotropic brownian rotations. Discontinuous distribution approach. *J. Chem. Phys.* 55:2399-2407.
- Yguerabide, J., M. A. Dillon, and M. Burton. 1964. Kinetics of diffusion-controlled processes in liquids. Theoretical consideration of luminescent systems: quenching and excitation transfer. *J. Chem. Phys.* 40:3040-3052.